INTERNATIONAL SOCIETY FOR
SOIL MECHANICS AND
GEOTECHNICAL ENGINEERING

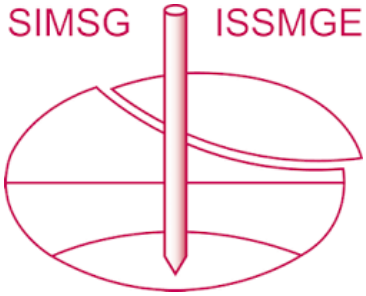

This paper was downloaded from the Online Library of the International Society for Soil Mechanics and Geotechnical Engineering (ISSMGE). The library is available here:

https://www.issmge.org/publications/online-library

This is an open-access database that archives thousands of papers published under the Auspices of the ISSMGE and maintained by the Innovation and Development Committee of ISSMGE.

The paper was published in the proceedings of the 7th International Conference on Earthquake Geotechnical Engineering and was edited by Francesco Silvestri, Nicola Moraci and Susanna Antonielli. The conference was held in Rome, Italy, 17 – 20 June 2019.

Earthquake Geotechnical Engineering for Protection and Development of Environment and Constructions – Silvestri & Moraci (Eds)
© 2019 Associazione Geotecnica Italiana, Rome, Italy, ISBN 978-0-367-14328-2

A two-wedge approach for the evaluation of seismic-induced rock-slides dams

G. Di Filippo, V. Bandini, G. Biondi & E. Cascone
University of Messina, Italy

ABSTRACT: In the framework of the Work Package WP2 of the 2017-18 Reluis project, focused on "Slope stability", the research group of Messina University proposed an analytical two-wedge methodology to evaluate the co-seismic performance of soil or rock slopes characterized by a sliding failure mechanism. The analysis accounts for the presence of a single internal joint and for the kinematic compatibility of the displacements of the two wedges which occurs along different segments of a two-planar sliding surface. A closed form solution, including the effect of the vertical component of ground motion, is provided for the evaluation of the slope yield acceleration coefficient k_y and for the displacement factor S which characterizes the equation of motion of the slope. The results of a parametric analysis are presented and discussed in the paper together with some useful charts providing k_y and S as a function of some non-dimensional geometrical and mechanical parameters.

1 INTRODUCTION

The analysis and prediction of seismic-induced effects on soil and rock slopes has received great attention in the last decades due to the well-documented disastrous consequences of several large earthquakes occurred worldwide.

In fact, during strong ground motions soils may experience large strains, pore water pressure build-up and cyclic degradation of mechanical properties that may significantly affect the stability conditions of natural slopes possibly triggering failures (e.g. Ishihara 1993; Biondi and Maugeri 2005) and causing large permanent displacements. Furthermore, as a consequence of severe ground motions, pore pressure build-up in rock joints and cyclic degradation of joint resistance may also occur producing or reactivating slope failures in rock masses along pre-existing discontinuities (Rodriguez et al. 1999, Bakun-Mazonr et al. 2013). Finally, for both soil and rock slopes, the possibly occurring large amplifications due to topographic irregularities may be also responsible or concurrent causes of earthquake-induced instabilities (e.g. Gazetas et al. 2002, Sepulveda et al. 2005, Rizzitano et al. 2014) and related damages.

Casualties, damages and economic losses are also frequently associated to the landslide effects on the post-seismic serviceability of road and railway networks which play a crucial role in the post-seismic scenario and in the emergency management of the stricken area (e.g. Biondi et al. 2004, Chiaro et al., 2015). As an example, among the 145 landslides triggered by the recent August 24, 2016 M_w = 6.0 Amatrice (Central Italy) earthquake (Lanzo et al. 2018, Stewart et al. 2017), which occurred over an area of approximately 500 km^2, more than 70% occurred in road-cuts and in some cases soil and rock mass movements produced roadway obstruction, aggravating the post-seismic emergency activities and the serviceability condition of the local road-net.

The characteristics of the earthquake-induced instabilities in rock slopes have been mainly related to the geomechanical properties and topographic features of the slope, to the orientation of the existing joint sets, to the presence of potentially unstable rock masses and, finally, to the shear resistance available along the rock-rock and soil-rock interfaces which bound the masses involved in a failure mechanism.

Most analytical methods of rock slope stability analysis rely on the classical limit equilibrium approach and allow accounting for some of these issues are. Hoek and Bray (1981) proposed an analytical method for plane failure analysis of rock slopes analyzing the case of horizontal upper slope surface and vertical tension crack. Inclined tension cracks were introduced by Sharma et al. (1995). Ling and Cheng (1997) described a limit equilibrium solution to evaluate the seismic safety factor as well as the yield acceleration and permanent displacements of the rock slope. In this solution the vertical component of the seismic acceleration is also accounted for. In recent studies (e.g. Cecconi et al. 2017), the effect of external loads transferred by anchors is also investigated. However, all the above-mentioned studies deal with a single rock block detached from the rock mass by a tension crack and the relevant equations do not differ signif-incantly from those usually adopted for the infinite slope scheme (e.g. Biondi et al. 2011).

In the framework of the Work Package 'WP2 - Slope stability' of the 2017-18 Reluis project, the research group of Messina University proposed a multi-wedge solution to evaluate the co-seismic performance of soil or rock slopes in the case of complex failure surface and joints internal to the mass involved in the failure mechanism. Some of the results of the research activities are summarized in the paper with reference to the case of a two-wedge analysis under 2D geometrical conditions. The results of a parametric analysis are also presented and discussed together with some useful charts which provide the horizontal component of the yield acceleration coefficient and all the factors involved in a Newmark-type analysis.

2 PROPOSED TWO-WEDGE APPROACH

The stability analyses addressed in this paper were carried out under 2D geometrical conditions using the limit equilibrium approach. The rock mass is divided into two blocks which move along two different segments of a bi-linear slip surface in a purely translational mode. In the analysis the equilibrium equations are satisfied in the horizontal and vertical directions, implying that the proposed approach is suitable to examine the failure mechanism of rock slopes sliding along slightly inclined surfaces. Furthermore, it is assumed that the rocks involved in the plastic mechanism behave as a perfectly plastic material obeying the Mohr–Coulomb failure criterion.

The reference slope scheme adopted in the analysis is described in Figure 1 together with the adopted notations. The driving and the resisting actions considered in the pseudo-static limit equilibrium conditions are shown in Figure 1a while Figure 1b describes the kinematic compatibility condition between the two blocks. Specifically:

- ϑ_{p1} and ϑ_{p2} denote the slope of the two segments describing the ground surface;
- ϑ_1 and ϑ_2 represent the dip of the two failure planes;
- β is the inclination to the vertical of the internal joint plane;
- H and L are the height and the total length of the slope considered in the analysis (the length B is also shown in the figure);
- k_h and k_v represent the horizontal and vertical components of the seismic coefficient;
- W_1 and W_2 are the weights of the two blocks;

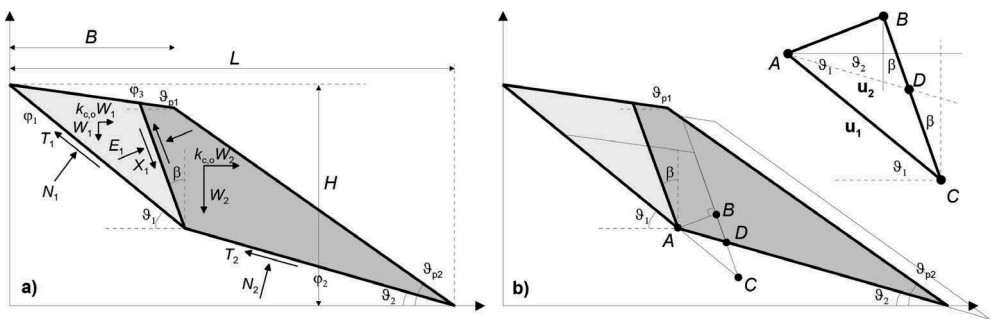

Figure 1. Reference slope scheme: a) driving and resisting forces; b) kinematic compatibility condition.

– T_1, T_2 and N_1, N_2 are the shear and the normal forces acting on each of the two blocks along the failure planes;
– X_1 and E_1 are the shear and the normal forces acting on the internal joint plane;
– φ_1, φ_2 and φ_3 are the angle describing the shear resistance available along the two segments of the failure planes (φ_1, φ_2) and the internal joint plane (φ_3);
– u_1 and u_2 are the displacement vectors describing the movements of each blocks along the direction of the sliding surface.

2.1 *Yield acceleration coefficient*

During the earthquake-induced motion of the two blocks system, the joint (inter-block) surface does not change its geometry and the shear strength along the slip and the joint surfaces is simultaneously fully mobilized. Accordingly, the yield acceleration coefficient k_y is unique for the two blocks, implying that the blocks start moving at the same time.

Since the whole rock mass consists of N= 2 blocks, the number of equilibrium equations available to examine the pseudo-static limit equilibrium condition is $2N = 4$ with 4 unknown variables: the normal forces N_1, N_2 and E_1 and a further variable consisting in the pseudo-static factor of safety F_{sd} (which can be estimated for given values of k_h and k_v) or in the horizontal component of the yield acceleration coefficient $k_{h,y}$ which can be estimated imposing $F_{sd} = 1$ for a given value of the ratio $\Omega = k_v/k_h$ between the vertical and the horizontal components of the seismic coefficients.

In the first case the solving set of equations is nonlinear and must be solved iteratively to estimate F_{sd}. Otherwise, a linear set of equations must be solved to derive $k_{h,y}$ and a close form solution can be obtained.

The set of equations to be solved in order to estimate $k_{h,y}$ is described in the Appendix together with the equations giving the four parameters α_1, α_2, α_3 and χ involved in the solution. Eqs. (1) and (2) provide the two closed form solutions obtained herein neglecting (eq. 1, $\Omega = 0$) or accounting for (eq. 2, $\Omega \neq 0$) the vertical component of the ground motion:

$$k_{y(\Omega=0)} = \frac{(\sin\alpha_1 - \sin\alpha_2) + \chi \cdot (\sin\alpha_3 - \sin\alpha_2)}{(\cos\alpha_1 + \cos\alpha_2) + \chi \cdot (\cos\alpha_3 + \cos\alpha_2)} \tag{1}$$

$$k_{y(\Omega\neq0)} = \frac{k_{y(\Omega=0)}}{1 + \Omega \cdot k_{y(\Omega=0)}} \tag{2}$$

2.2 *Equation of motion and displacement factors*

The failure mechanism assumed in the analysis requires the two adjacent blocks, delimited by the straight-line segments describing the slip surface, to be rigidly connected to avoid any separation or overlapping at the contact of their bases with the slip surface and along the joint surface. Since the slip and the joint surfaces remain fixed throughout sliding, the kinematic compatibility condition (i.e. no separation or overlapping with the slip surfaces and along the joint surface) implies that for the two adjacent blocks (with base inclination ϑ_1 and ϑ_2)the component of displacements u_1 (segment AC in Figure 2b) and u_2 (segment AD in Figure 2b) along the normal to the joint surface (segment AB in Figure 2b)coincide (eq. 3):

$$AB = u_1 \cdot \cos(\beta + \vartheta_1) = u_2 \cdot \cos(\beta + \vartheta_2) \tag{3}$$

Eq. (3) allows expressing the displacement u_2 of the *block 2* as a function of the displacement u_1 of the *block 1* (assumed as a reference in the displacement analysis) by introducing a conversion factor q:

$$u_2 = \frac{\cos(\beta + \vartheta_1)}{\cos(\beta + \vartheta_2)} \cdot u_1 = q \cdot u_1 \tag{4}$$

The equations of relative motion of the two blocks can be obtained by equating the unbalanced forces, acting parallel to the block bases, to the inertial forces acting on the blocks

during the motion. The solving set of equations is provided in the Appendix and allows to derive the following expressions of the two equations of motion:

$$\begin{aligned} \ddot{u}_1 &= S_1 \cdot \left(k_h - k_{h,y}\right) \cdot g \\ \ddot{u}_2 &= S_2 \cdot \left(k_h - k_{h,y}\right) \cdot g \end{aligned} \tag{5}$$

In eq. (5) S_1 and $S_2 = q \cdot S_1$ are displacement factors depending on all the parameters describing the overall slope geometry (ground and slip surfaces) and the shear strength available along the external slip surface and internal joint surface.

As for the yield acceleration coefficient, a closed form solution has been also derived to compute S_1 neglecting (eq. 6) or accounting (eq. 7) for the vertical component of the ground motion:

$$S_{1\,(\Omega=0)} = \frac{(\cos\alpha_1 + \cos\alpha_2) + \chi \cdot (\cos\alpha_3 + \cos\alpha_2)}{[\cos(\alpha_1 + \vartheta_1) + \cos(\alpha_2 - \vartheta_1)] + q \cdot \chi \cdot [\cos(\alpha_3 + \vartheta_2) + \cos(\alpha_2 - \vartheta_2)]} \tag{6}$$

$$S_{1\,(\Omega\neq 0)} = S_{(\Omega=0)} \cdot \left(1 + \Omega \cdot k_{y(\Omega=0)}\right) \tag{7}$$

2.3 *Comparison with literature*

The proposed approach provides a general solution for a two-block scheme of analysis. To validate the proposed method of analysis comparisons for particular cases were carried out imposing, when necessary, that the two-wedge mechanism degenerates into a single block mechanism. The pseudo-static analysis proposed herein can be also put in the framework of the well-known method of slices for the limit equilibrium stability analysis of slopes. Specifically, all the solutions presented herein for the computation of the yield acceleration coefficient $k_{h,y}$ and of the displacement factor S_1 can be compared with the solutions that can be derived using the General Limit Equilibrium method and the Janbu's Simplified Method and with some solutions already available in the literature with reference to planar failure mechanism.

In the General Limit Equilibrium (GLE) formulation, the equilibrium of forces can be considered assuming a vertical inter-block boundary (β=0) and an interslice force function $f(x) = \tan(\varphi_3)$. In the Janbu's Simplified Method a vertical inter-block boundary (β=0) can be considered neglecting the interslice shear forces (φ_3=0); while for theplanar surface assumed by Ling & Cheng (1997) $k_{h,y}$ and S_1 can be evaluated assuming $\vartheta_1 \neq \vartheta_2$, $\varphi_1=\varphi_2=0$, $\beta=\pi/2 - \vartheta_1$ and W_1=0 which implies that the two-block system degenerates into a single-block system. Table 1 summarizes the solutions described above (obtained neglecting the vertical component of the ground motion) in terms of yield acceleration coefficient k_y and displacement factor S.

It can be observed that in all the examined cases the solving equations provided by the present method coincide with those of the other considered limit equilibrium methods.

3 PARAMETRIC ANALYSIS

The parametric analysis illustrated and discussed in this paper aims to investigate the effect of the inclination β of the joint surface on the computed values of the yield acceleration coefficient $k_{h,y}$ and on the factors S_1 and q.

To this purpose the closed form solutions giving the normal forces N_1 (eq. 8), N_2 (eq. 9) and E_1 (eq. 10) must be introduced. Herein, these solutions are provided for the case $\Omega = 0$ and the same condition is considered in the parametric analysis:

$$N_{1(\Omega=0)} = \frac{(W_1 + W_2) \cdot [\cos(\alpha_1 + \vartheta_1) + \cos(\vartheta_1 - \alpha_2)]}{(\cos\alpha_1 + \cos\alpha_2) + \chi \cdot (\cos\alpha_3 + \cos\alpha_2)} \tag{8}$$

$$N_{2(\Omega=0)} = \frac{(W_1 + W_2) \cdot \chi \cdot [\cos(\alpha_3 + \vartheta_2) + \cos(\vartheta_2 - \alpha_2)]}{(\cos\alpha_1 + \cos\alpha_2) + \chi \cdot (\cos\alpha_3 + \cos\alpha_2)} \tag{9}$$

Table 1. Comparison with literature

Reference schemes	Assumptions and solutions
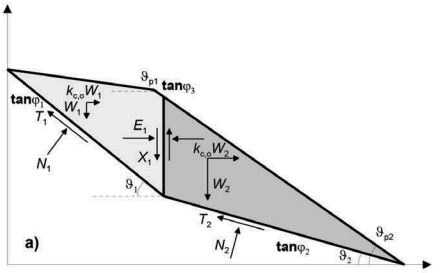	General Limit Equilibrium (GLE) $\varphi_1 \neq \varphi_2 \neq \varphi_3 \neq 0$ $\vartheta_1 \neq \vartheta_2 \quad \beta = 0$ k_y from eq. (1) S from eq. (6)
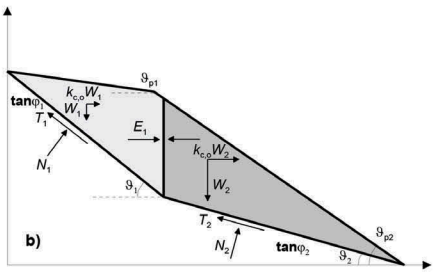	Janbu's Simplified Method $\varphi_1 \neq \varphi_2 \quad \varphi_3 = 0$ $\vartheta_1 \neq \vartheta_2 \quad \beta = 0$ $k_{y(\Omega=0)} = \dfrac{\tan(\varphi_1 - \vartheta_1) + \chi \cdot \tan(\varphi_2 - \vartheta_2)}{1+\chi}$ $S_{(\Omega=0)} = \dfrac{1+\chi}{\dfrac{\cos\varphi_1}{\cos(\varphi_1 - \vartheta_1)} + q \cdot \chi \cdot \dfrac{\cos\varphi_2}{\cos(\varphi_2 - \vartheta_2)}}$
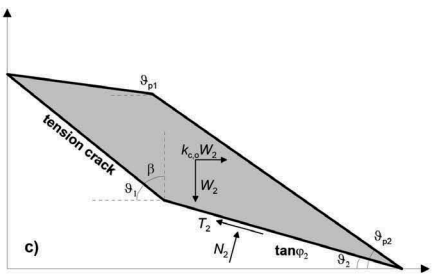	Planar surface analysis $W_1 = 0$ $k_{y(\Omega=0)} = \tan(\varphi_2 - \vartheta_2)$
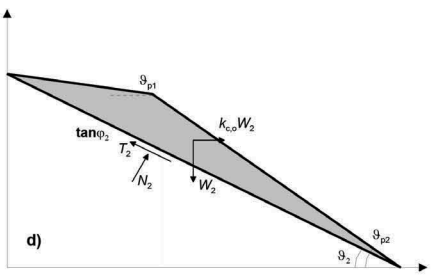	Planar surface analysis $W_1 = 0$ $k_{y(\Omega=0)} = \tan(\varphi_2 - \vartheta_2)$ $S_{(\Omega=0)} = \dfrac{\cos(\varphi_2 - \vartheta_2)}{\cos\varphi_2}$

Note: the equations giving α_1, α_2, α_3 (which appear in eqs.1 and 6), χ and q are given in the appendix.

$$E_{1(\Omega=0)} = \frac{W_2 \cdot [\sin(\beta - \alpha_1) - \sin(\beta - \alpha_3)]}{(\cos\alpha_1 + \cos\alpha_2) + \chi \cdot (\cos\alpha_3 + \cos\alpha_2)} \tag{10}$$

In order to avoid tensile stress within the rock-slope, the values of the aforementioned actions must be positive whatever is the angle β. It can be demonstrated that only the influence of β on the normal action N_1 is relevant to check this condition.

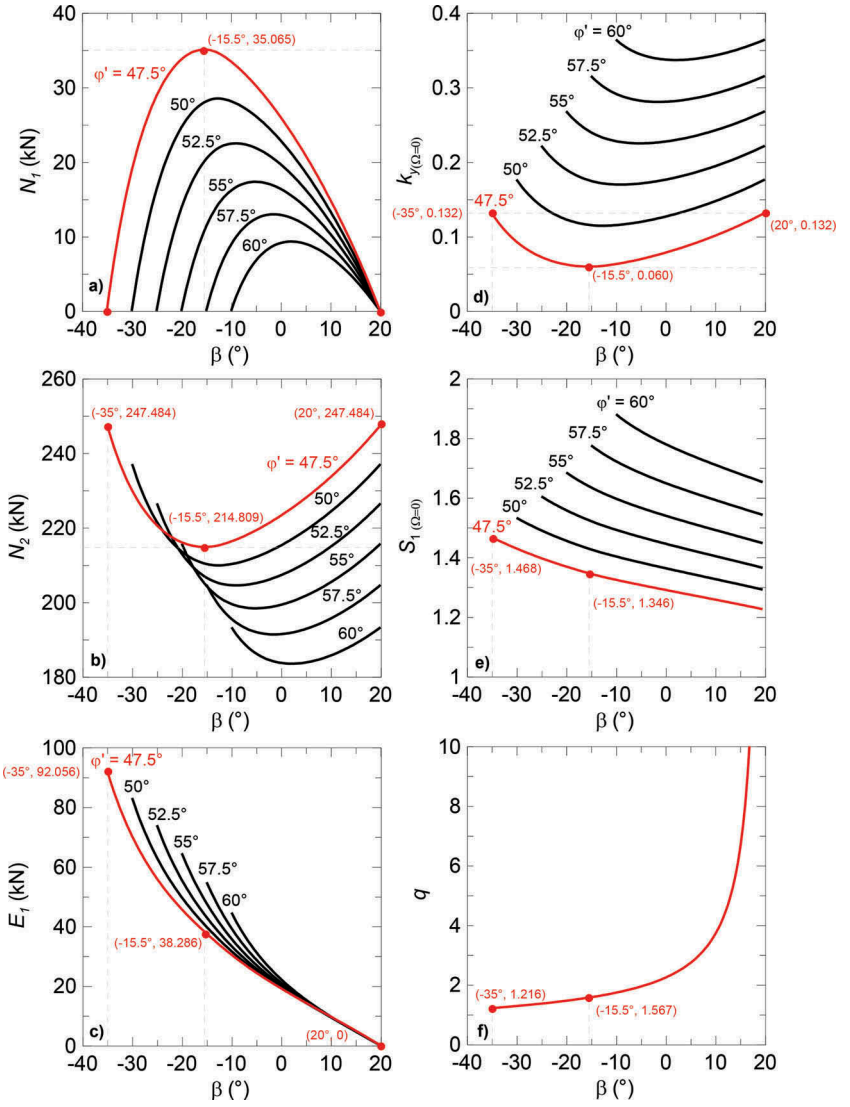

Figure 2. (a) normal force N_1, (b) normal force N_2, (c) interslice normal forces E_1, (d) critical acceleration coefficient $k_{y\ (\Omega=0)}$, (e) displacement factor $S_{(\Omega=0)}$, (f) displacement conversion factor q,(ϑ_1=70°, ϑ_2=40°, φ'_1=φ'_2=φ'_3, Ω=0, B/H=0.25, ϑ_{2p}=60°, L/H=0.827, ϑ_{1p}=0).

As an example, for the case ϑ_1 = 70°, ϑ_2 = 40°, φ'_1 = φ'_2 = φ'_3 = φ', ϑ_{2p}=60°, ϑ_{1p}=0 and H = 8m (B/H=0.25 and L/H=0.827), Figure 2 shows the influence of the joint inclination β on the values of forces N_1, N_2 and E_1 (Figure 2 a-c) and on the values of the yield acceleration coefficient $k_{h,y}$ and of the factors S_1 and q. (Figure 2 d-f).

From Figure 2a it can be observed that N_1 is positive within a certain interval of values of β; in the same range, the actions N_2 (Figure 2b) and E_1 (Figure 2c) always take positive values.

Using eq. (8) it can be demonstrated that the values of β which implies the condition $N_1 > 0$ range between $\beta_1 = \varphi'_2 + \varphi'_3 - \vartheta_2 - \pi/2$ and $\beta_2 = \pi/2 - \vartheta_1$. The equations giving $k_{h,y}$ and S_1 for the cases $\beta = \beta_1$ and $\beta = \beta_2$ are summarized in Table 2.

For the slope scheme considered in Figure 2 it is β_1 = -35° and β_2 = 20°. For $\beta = \beta_1$ = -35° the rock-slope consists of two different blocks ($W_1 \neq 0$, $W_2 \neq 0$) and it is N_1 = 0 (Figure 2a), N_2 = 247.5kN (Figure 2b), E_1 = 92.0 kN (Figure 2c), $k_{h,y}$ = 0.132 (Figure 2d) and S_1 = 1.5 (Figure 2e). If $\beta = \beta_2$ = 20° the rock-slope consists of a single block (W_1 = 0, $W_2 \neq 0$, Table 1 - case *c*) the

Table 2. Particular cases for the evaluation of k_y and S

β	k_v	N_2	E_1	S_1
$\beta=\beta_1$	$\tan(\phi_2 - \vartheta_2)$	$(W_1 + W_2)\frac{\cos\phi_2}{\cos(\phi_2-\vartheta_2)}$	$W_1\frac{\cos\phi_3}{\cos(\phi_2-\vartheta_2)}$	$\frac{\cos(\phi_2-\vartheta_2)}{\cos\phi_2}$
$\beta_1=\beta_2$	$\tan(\phi_2 - \vartheta_2)$	$W_2\frac{\cos\phi_2}{\cos(\phi_2-\vartheta_2)}$	0	-

displacement factor S_1 cannot be evaluated and it is $N_1 = E_1 = 0$ (Figure 2 a, c) and, since the overall weight of the slope $W = W_2$ is invariant with β, it is again $N_2 = 247.5$ kN (Figure 2b). In the cases $-35° = \beta_1 < \beta < \beta_2 = 20°$ $k_{h,y}$ and N_2 exhibit a minimum value while N_1 attains a maximum for $\beta = -15.5°$; in this case it is $k_{h,y}$=0.06 (Figure 2d), N_1=35.1kN (Figure 2a), E_1=38.3 kN (Figure 2c), N_2=214.8 kN (Figure 2b); the displacement factor (eq. 6) is equal to 1.346 (Figure 2e).

As shown in the appendix A, the factor q does not depend on the shear resistance mobilization along the interfaces and it is an increasing function of β (Figure 2f); the displacement factor $S_2 = S_1 \bullet q$ (eq. 5) allows the evaluation of the displacements for the *block 2*. As it can be observed from the plots of Figure 2, the influence of the angle β on the computed values of the yield acceleration coefficient and of the displacement factors is extremely relevant.

4 CONCLUSION

This paper describes a 2D two-wedge approach for the evaluation of seismic-induced rockslides using the limit equilibrium method. The analytical solution is presented in terms of yield acceleration coefficient and displacement factor, neglecting or considering the vertical component of the seismic acceleration. The results obtained for some particular cases were compared with solutions available in the literature with reference to planar failure mechanisms.

The parametric analysis illustrated and discussed in the paper aims to investigate the effect of the inclination β of the internal joint plane on the computed values of the yield acceleration coefficient $k_{h,y}$ and on the displacement factors S_1 and q, fixing the sliding surface (ϑ_1 and ϑ_2) and assuming Ω=0.

The study shows the existence of a critical inclination of the internal joint plane at which the yield acceleration assumes a minimum value; the inclination of the internal joint plane and the minimum value of yield acceleration are functions of the shear resistance available along the two segments of the failure planes (φ_1, φ_2) and the internal joint plane (φ_3). It is worth noting that, though results refer to the case in which the same values of the angle of shear resistance is assumed along the internal joint and external sliding surfaces, the solution provided by equation 2 is valid for any combination of φ_1, φ_2 and φ_3.

ACKNOWLEDGEMENT

This work is a part of the research activities carried out by the Messina Research Unit in the framework of the work package WP2-Slope Stability of a Research Project funded by the ReLuis (University Network of Seismic Engineering Laboratories) consortium.

REFERENCES

Biondi G. & Maugeri M., 2005. Seismic response analysis of Monte Po hill (Catania). Advances in Earthquake Engineering. Vol. 14, 2005: 177-195.

Biondi G., Condorelli A., Maugeri M. & Mussumeci G., 2004. Earthquake-triggered landslide hazards in the Catania area. Management Information Systems, Vol. 9, 1 January 2004: 115-130.

Biondi G., Cascone E, Rampello G. 2011 - Valutazione del comportamento dei pendii in condizioni sismiche - Rivista Italiana di Geotecnica 2011.

Cecconi M., Cencetti C., Melelli L., Pane V. & Vecchietti A., 2017. Non-dimensional analysis for rock slope plane failure in seismic (pseudostatic) conditions. Bull. Engineering Geology and the Environment

Chiaro G., Kiyota R., Pokhrel R. M., Goda K., Katagiri T. & Sharma K., 2015. Reconnaissance report on geotechnical and structural damage caused by the 2015 Gorkha Earthquake, Nepal. Soils and Foundations, 55 (5): 1030-1043, October 2015.

Gazetas G., Kallou P.V. & Psarropoulos P. N., 2002. Topography and soil effects in the MS 5.9 Parnitha (Athens) earthquake: the case of Adámes. Natural Hazards, 2002; 27(1-2): 133-169.

Hoek E, Bray J. 1981. Rock slope engineering, 3rd edn. The Institution of Mining and Metallurgy, London

Lanzo, G., Tommasi, P., Ausilio, E., Aversa, S., Bozzoni, F., Cairo, R., d'Onofrio, A., Durante, M.G., Foti, S., Giallini, S., Mucciacciaro, M., Pagliaroli, A., Sica, S., Silvestri, F., Vessia, G., and Zimmaro, P., 2018. Reconnaissance of geotechnical aspects of the 2016 Central Italy earthquakes. Bulletin of Earthquake Engineering. DOI: 10.1007/s10518-018-0350-8.

Ling, H.I., Cheng, A.H.D., 1997. Rock sliding induced by seismic force. Int. J. Rock Mech. Min. Sci. 34 (6), 1021–1029.

Rizzitano S., Cascone E. & Biondi G., 2014. Coupling of topographic and stratigraphic effects on seismic response of slopes through 2D linear and equivalent linear analyses. Soil Dynamics and Earthquake Engineering 67: 66-84.

Rodríguez C., Bommer J. & Chandler R., 1999. Earthquake-induced landslides: 1980–1997. Soil DynEarthq Eng. 1999;18(5):325–346. http://dx.doi.org/10.1016/S0267-7261(99) 00012-3.

Sharma S., Raghuvanshi T.K., Anbalagan R., 1995. Plane failure analysis of rock slopes, Geotechnical and Geological Engineering, 13: 105-111.

Sepulveda S. A., Murphy W., Jibson R. W. & Petley D.N., 2005. Seismically induced rock slope failures resulting from topographic amplification of strong ground motions: The case of Pacoima Canyon, California. Engineering Geology 80 (2005) 336–348.

Stewart J.P., Lanzo G., Alexander N., Aversa S., Bozzoni F., Castiglia M., Chiabrando F., Chiaradonna A., D'Onofrio A., Dashti S., De Risi R., De Silva F., Di Pietra V., Di Sarno L., Durante M.G., Falcucci E., Foti S., Fragiadakis M., Franke K., Galadini F., Giallini S., Gori S., Grasso N., Katsiveli E., Kayen R.E.,Kishida T., Mucciacciaro M., Mylonakis G., Pagliaroli A., Pelekis P., Penna A., Psycharis I., Reimschiissel B., Santucci de Magistris F., Scasserra G, Sextos A., Sica S., Silvestri F., Simonelli A. L., Tommasi P., Tropeano G., Vintzilaiou E., &Zimmaro P., 2017. Engineering reconnaissance following the August 24, 2016 M6.0 Central Italy earthquake. 16WCEE 2017. Santiago, Chile.

APPENDIX

With reference to the slope scheme described in Figure 1, this appendix provides the systems of equations to be solved in order to evaluate the yield acceleration coefficient and the displacement factors involved in a Newmark-type analysis.

Evaluation of k_y

$$\begin{bmatrix} N_1 \\ N_2 \\ k_y \\ E_1 \end{bmatrix} \begin{bmatrix} \tan\phi_1 \cos\vartheta_1 - sen\vartheta_1 & 0 & -W_1 & \tan\phi_3\, sen\beta + \cos\beta \\ \tan\phi_1\, sen\vartheta_1 + \cos\vartheta_1 & 0 & \Omega W_1 & \tan\phi_3 \cos\beta - sen\beta \\ 0 & \tan\phi_2 \cos\vartheta_2 - sen\vartheta_2 & -W_2 & -\tan\phi_3\, sen\beta - \cos\beta \\ 0 & \tan\phi_2\, sen\vartheta_2 + \cos\vartheta_2 & \Omega W_2 & -\tan\phi_3 \cos\beta + sen\beta \end{bmatrix} = \begin{bmatrix} 0 \\ W_1 \\ 0 \\ W_2 \end{bmatrix} \tag{11}$$

Evaluation of S_1

$$\begin{bmatrix} N_1 \\ N_2 \\ k_y \\ E_1 \end{bmatrix} \begin{bmatrix} \tan\phi_1 \cos\vartheta_1 - sen\vartheta_1 & 0 & -W_1 & \tan\phi_3\, sen\beta + \cos\beta \\ \tan\phi_1\, sen\vartheta_1 + \cos\vartheta_1 & 0 & \Omega W_1 & \tan\phi_3 \cos\beta - sen\beta \\ 0 & \tan\phi_2 \cos\vartheta_2 - sen\vartheta_2 & -W_2 & -\tan\phi_3\, sen\beta - \cos\beta \\ 0 & \tan\phi_2\, sen\vartheta_2 + \cos\vartheta_2 & \Omega W_2 & -\tan\phi_3 \cos\beta + sen\beta \end{bmatrix} = \begin{bmatrix} 0 \\ W_1 \\ 0 \\ W_2 \end{bmatrix} \tag{12}$$

Relevant notations

$$\begin{cases} \alpha_1 = \beta + \phi_1 - \phi_2 - \phi_3 - \vartheta_1 + \vartheta_2 \\ \alpha_2 = \beta - \phi_1 - \phi_2 - \phi_3 + \vartheta_1 + \vartheta_2 \\ \alpha_3 = \beta - \phi_1 + \phi_2 - \phi_3 + \vartheta_1 - \vartheta_2 \end{cases} \chi = \frac{W_2}{W_1}\ q = \frac{\cos(\beta + \vartheta_1)}{\cos(\beta + \vartheta_2)} \tag{13}$$